DUCTILE-BRITTLE TRANSITION FOR REINFORCED CONCRETE BEAMS: EXPERIMENTAL AND NUMERICAL INVESTIGATION

C. Bosco[1], A. Carpinteri[1], M. El-Khatieb[1] and G. Ferro[1]

A brief presentation is given of the experimental results on RC beams in order to evaluate the scale dependence of plastic rotational capacity, the minimum reinforcement and the existence of transitional phenomena of failure. The experimental investigation was planned in a Round Robin proposed by the ESIS Technical Committee 9 on Concrete; 45 RC beams were tested varying scale, percentage of reinforcement and slenderness.

The results presented in this paper concern only one beam geometry, while the attention is focused on the influence of steel percentage. The applied force vs. deflection diagrams are presented together with the experimental load vs. plastic rotation diagrams and compared with the numerical simulations.

INTRODUCTION

Reinforced concrete beams undergo different failure mechanisms by varying steel percentage and/or beam slenderness and/or beam size-scale (in the last variation, the steel percentage being constant). The three fundamental collapse mechanisms are the following:
-nucleation and propagation of cracks at the edge in tension;
-compression and crushing at the edge in compression;
-formation of inclined shear cracks.

As regards tensile failures, the minimum amount of reinforcement can be determined through the concepts of fracture mechanics (1-3), while the maximum inelastic rotational capacity can be obtained even when failure shifts to compressive sides. Both such quantities were found as subjected to remarkable size effects. An extensive experimental research was proposed by ESIS Technical Committee 9 on Concrete in order to obtain a rational and unified explanation for the transitions usually obtained between the above mentioned collapse mechanisms.

The influence of size on the inelastic rotational capacity has not been completely clarified (and demonstrated) yet. In fact the experimental data available up to a few years ago, mostly obtained by load controlled tests on reinforced concrete beams

[1]Politecnico di Torino, Dept. of Structural Engineering, 10129 Torino, Italy.

with high ductility bars, show a considerable scatter. On the other hand, some numerical evaluations, assuming strain localization in the compression zone, indicate that plastic rotation depends on the scale (beam depth) and the experimental tests recently carried out, seem to validate this dependence (4,5).

In this paper the attention is focused onto the transition of failure mechanism (from reinforcement failure to crushing of concrete) and plastic rotation evaluation varying the amount of reinforcement and keeping beam cross-section and slenderness constant.

A numerical simulation of the tests was performed. The results presented were obtained using a specific FE program (6), particularly aimed to the object of the present investigation.

EXPERIMENTAL DETAILS

Three point bending tests, were carried out at the Department of Structural Engineering of the Politecnico di Torino, on 45 reinforced concrete beams. Three values of slenderness L/h=6, 12, 18 (span to depth ratio) were taken into account. The beams were subdivided into three series, according to the different cross-sections: (A) 100x100 mm, (B) 100x200 mm and (C) 200x400 mm, while the effective depth to total depth ratio d/h was equal to 0.9. The beams were reinforced only in tension with five different percentages: 0.12%, 0.25%, 0.5%, 1.0% and 2.0%. All the beams were cast from the same batch and no shear reinforcement in the central part of the beams was provided.

TABLE 1 - Geometrical characteristics and percentages of steel reinforcement of beams whose results are presented in this paper.

beam	tension reinforcement	$A_s/(bh)$
B025-06	1 ϕ 8	0.25
B050-06	2 ϕ 8	0.50
B100-06	4 ϕ 8	1.00
B200-06	2 ϕ 16	2.00

A closed-loop servo-controlled testing machine was used. The tests were performed in displacement control for the beams with pecentage of reinforcement greater than 0.50%, while for the others the crack mouth opening displacement (CMOD) control was used, in order to avoid sudden failure in the event of snap-back phenomena occurring. Top and bottom edge deformation were measured by means of potentiometric transducers with gauges of length equal to the depth of the beam, placed at 1/10 of the depth of the cross-section from both the beam extrados and intrados. The transducers had a 20 mm measuring range, while vertical displacements were measured by means of two transducers placed at midspan. Two additional transducers were used to measure the settlements at supports, so the real value of the midspan deflection was obtained by subtracting the average readings at supports from the average readings at midspan. The end supports consisted in a fixed hinge and a roller enabling

the beam to move horizontally. The load was transferred onto the beams by means of a platen having a length equal to half the beam depth.

The compressive strength of concrete was obtained from 8 cubic specimens measuring 100 mm in side and the average value f_{cm} was 48.2 N/mm^2. The elastic modulus of concrete was determined from four specimens measuring 100x100x300 mm, which provided an average value equal to 35,000 N/mm^2. The fracture energy of concrete, determined according to RILEM draft recommendation on six specimens, had an average value $\mathcal{G}_F$ equal to 0.115 N/mm. The critical value of stress-intensity factor can then be evaluated as:

$$K_{IC} = \sqrt{\mathcal{G}_F E} = 63.4 \ \mathrm{N\,mm^{-\frac{3}{2}}} \tag{1}$$

The steel bars had nominal diameters of 4, 8 and 16 mm, respectively. The 4 mm bars did not exhibit well-defined yield point and conventional yield limit, obtained from the stress-strain curve at 0.2% of permanent deformation, was equal to 604 N/mm^2. On the other hand, the yield strength for the bars of 8 and 16 mm, equalled 643 N/mm^2 and 518 N/mm^2, respectively.

EXPERIMENTAL RESULTS

In what follows, we consider only the tests performed on the beams of class B with cross-sectional area equal to 100x200 mm and slenderness L/h = 6. The values of the experimental parameters obtained for the four considered beams of class B are reported in Table 2.

TABLE 2 - Experimental load, deflections and rotations for the four beams of class B.

beam	Yielding load (kN) P_y	Peak load (kN) P_p	Ultimate load (kN) P_u	Midspan deflection at peak load (mm) δ_p	Plastic rotation at peak load θ_p	Ultimate rotation θ_u
B025-06	21.70	22.95	20.66	5.18	0.00891	0.0179
B050-06	39.47	41.85	37.66	7.22	0.0113	0.0221
B100-06	76.74	83.00	74.70	12.62	0.00431	0.00634
B200-06	79.48	107.53	102.38	5.36	0.00106	0.00163

Plastic rotation definition is often related to the calculation method adopted for the analysis of statically indeterminate structures. Eurocode 2 and Model Code 1990 (7), state that plastic rotation θ_p may be obtained by integration, along the plastic zone l_p (where the stress in the tensile reinforcement is higher than its yield limit), of the difference between mean curvature $\frac{1}{r_m}$ and the curvature obtained at the yield limit of steel, $\frac{1}{r_{my}}$:

$$\theta_p = \int_{l_p} (\frac{1}{r_m} - \frac{1}{r_{my}}) \mathrm{d}z. \tag{2}$$

In the relationship (2) the curvatures are worked out from the ratio between the difference of the average strain ϵ_{sm} of the tension chord and the average strain ϵ_{cm} at

the compression one and 0.8 h, being the measurements given by the potentiometric transducers placed at h/10 from the upper and lower beam edges.

Ultimate rotation θ_u was taken at the moment corresponding to 90% of maximum bending moment as determined at the softening branch that precedes failure. When the latter value was not reached, the failure value was used instead. Ultimate load P_u was taken from the experimental results with the same criteria adopted for the ultimate rotation.

In Figure 2 the load versus plastic rotation diagrams are given for the four considered beams. Each curve is plotted up to the end of the experimental test and both the peak and ultimate plastic rotation are indicated on it.

From Figure 2 is easy to observe the difference of ductility shown by the four beams. For the B025-06 and B050-06 types, in particular, plastic rotation is considerable higher than the values shown by the other two beams. It is worth noting that in the first three beams plastic rotation is obtained at 90% of the maximum applied load in the descending branch of the load-deflection curve, while the B200-06 beam shows the crushing of concrete in the compressive zone before the 90% of the peak load could be reached.

In the latter case, it is necessary to observe that plastic rotation is very limited and practically negligible. On the other hand, strictly referring to relationship (2), in this case plastic rotation must be assumed as equal to zero. It is however necessary to take into account that sometimes inelastic rotation is observed even though yielding limit of steel is not reached or it is just overtaken.

In such cases however a conventional value of permanent deformation on the load versus deflection diagram could be defined (deviation from linearity) and the inelastic rotation obtained by a relationship of type (2) again. The yielding load given in Table 2 for beam B200-06 was conventionally defined as stated above.

From a qualitative point of view, it is necessary to remark that plastic rotation (and more generally ductile behaviour) increases with increasing the percentage of tensile reinforcement, up to a certain value, and then decreases for further increments of reinforcement. This way of describing the phenomenon is equivalent to the statement given by CEB, in which plastic rotation diagram is expressed versus the neutral axis depth ratio x/d, x and d being the compression depth at ultimate limit state and the effective depth of the beam, respectively.

For the numerical simulations, performed with the FE code (6) and reported as dotted lines in Figure 1, the nonlinear softening constitutive law by Hordijk (8) was used. The program adopts the smeread crack approach for modeling of cracks; the simulations were performed by using the fixed crack model and were conducted in displacement control. The mesh used for the simulations consisted in 100 elements and 120 nodes, while the Newton-Raphson method was selected to solve the equilibrium equations.

From Figure 1, it is possible to observe how the simulations are in a good agreement with the experimental load versus deflection curves, up to the yielding of steel. The subsequent parts of the load-deflection curves are strictly influenced by the parameters governing the concrete constitutive law. In particular, for the beam B200-06, the numerical load versus deflection curve shows a very brittle behaviour due to di-

agonal tension mode, showing a crushing failure of concrete in the compression zone. This brittleness could be due to the mesh adopted, although at the moment the mesh-dependence of the strucural response has not been analysed.

CONCLUSIONS

From an extensive experimental investigation aimed at verifying the existence f transitional phenomena of failure and scale effects in reinforced concrete beams, a first series of results was considered. For a given beam slenderness and cross-sectional geometrical characteristics, the percentage of reinforcement was assumed as variable and the following results were obtained:

- for low percentage of reinforcement (low values of the x/d ratio) failure occurs at the edge in tension and is affected by steel characteristics;
- with increasing the content of steel, failure shifts from the lower side to the upper side of the beam and crushing of concrete prevails;
- plastic rotation shows a characteristic two-branches trend with slopes of opposite sign (positive slope from very low to intermediate content of steel and negative slope with higher percentage of reinforcement).

As regards the numerical simulation by using a FE code, the authors can affirm that a good agreement was found with the experimental results, up to the yielding of steel. The subsequent parts of the load-deflection curves for the four considered cases were numerically obtained with a satisfactory agreement depending on the choice of the several parameters describing the softening behaviour of concrete.

REFERENCES

(1) Carpinteri, A., J. Struct. Eng., (ASCE), Vol. 110, 1984, pp. 544-558.

(2) Bosco, C., Carpinteri, A. and Debernardi, P.G., J. Struct. Eng., (ASCE), 1990, Vol. 116, pp. 427- 437.

(3) Bosco, C. and Carpinteri, A., J. Eng. Mechanics (ASCE), Vol.118, 1992, pp 1564-1577.

(4) Bosco, C.,Carpinteri, C., and Debernardi, P.G. "Scale effect on plastic rotational capacity of r.c. beams", in Fracture Mechanics of Concrete Structures, Breckenridge, Edited by Z.P. Bažant, Elsevier Applied Science, London, 1992, pp.735-740.

(5) Bosco, C. and Debernardi, P.G. "Experimental investigation on the ultimate rotational capacity of r.c. beams", Internal Report n.36, Dept. of Structural Engineering, Politecnico di Torino - June 1992.

(6) SBETA Program Documentation, Prague, 1992.

(7) Comitée Euro-International du Béton (C.E.B.), Model Code 1990.

(8) Hordijk, D. A. "Local approach to fatigue of concrete", Doctoral Thesis, Technische Universiteit Delft, 1991.

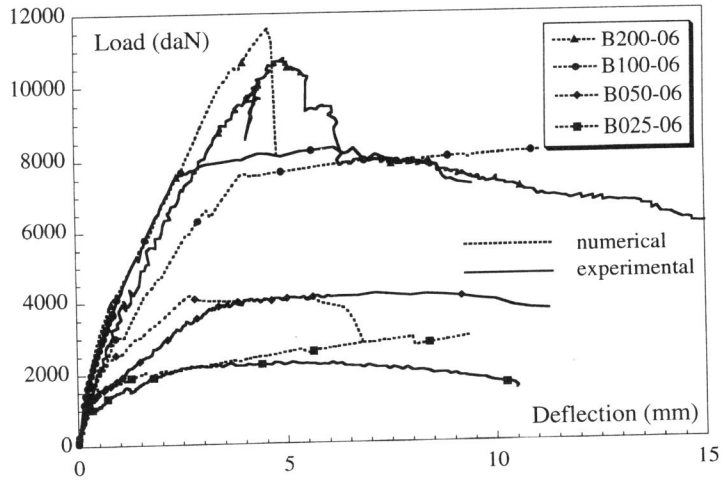

Figure 1: Experimental diagrams versus numerical simulations.

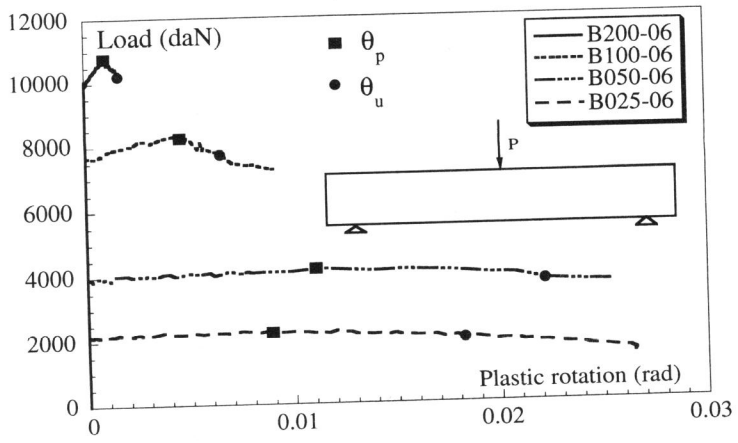

Figure 2: Load versus plastic rotation for the four considered beams.